INSTITUTE OF PHYSICS PUBLISHING JOURNAL OF PHYSICS: CONDENSED MATTER

J. Phys.: Condens. Matter **18** (2006) 5655–5668 doi:10.1088/0953-8984/18/24/007

Radiolysis of NaCl at high and low temperatures: development of size distribution of bubbles and colloids

A A Turkin[1], A V Sugonyako[2], D I Vainshtein[2] and H W den Hartog[2,3]

[1] National Science Centre Kharkov Institute of Physics and Technology, 61108 Kharkov, Ukraine
[2] Solid State Physics Laboratory, University of Groningen, 4 Nijenborgh 9747 AG Groningen, The Netherlands

E-mail: a.turkin@kipt.kharkov.ua, a.v.sugonyako@rug.nl, d.i.vainchtein@rug.nl and h.w.den.hartog@rug.nl

Received 18 January 2006, in final form 10 April 2006
Published 2 June 2006
Online at stacks.iop.org/JPhysCM/18/5655

Abstract

New experimental results are presented on low temperature irradiation (18 °C) of rock-salt samples which had been exposed to initial doses up to 320 GRad at 100 °C. Differential scanning calorimetry (DSC) shows that the latent heat of melting (LHM) of sodium colloids decreases during subsequent low-temperature irradiation, whereas the stored energy (SE) increases slowly, indicating that the process of radiolysis continues. The decrease of the LHM is due to dissolution of large colloids, because the intensities of the melting peaks decrease during the second stage irradiation at low temperature. The model is formulated to describe the nucleation kinetics and the evolution of the size distribution of chlorine precipitates and sodium colloids in NaCl under high dose irradiation. It is shown that the mechanism of dissolution of large Na colloids during low temperature irradiation can be related to melting of sodium colloids.

1. Introduction

The problem of radiation damage formation in synthetic and natural NaCl samples has attracted the attention of researchers, since rock-salt is a prominent candidate medium for storage of high level radioactive waste [1, 2]. Irradiation of NaCl crystals with electrons of moderate energies (e.g. ∼1 MeV) or gamma rays causes electronic excitations that produce H and F centres (Frenkel pairs) in the halide sub-lattice, whereas the cation sub-lattice is not affected significantly in the primary process. Agglomeration of H centres and F centres [3–5] results in the formation of chlorine bubbles and Na-precipitates, respectively.

The majority of the models describing radiolysis in NaCl are based on the Jain–Lidiard model [4, 5], according to which the dislocation bias for H centres is the driving force for the

[3] Author to whom any correspondence should be addressed.

colloid growth in alkali halides, just as in the case of void growth in metals under irradiation. However, the processes of radiation damage formation in ionic compounds are quite different from those in metals, because the primary radiolytic displacements occur only in one sublattice and the primary point defects, H and F centres, keep their chemical identities during diffusion and agglomeration. For this reason these models are not able to explain a number of important features of damage formation in NaCl which we have found during our investigations. We have observed experimentally [6–8] that in heavily irradiated NaCl samples (i) no saturation of radiation damage with dose is observed and (ii) relatively large vacancy voids can form together with radiolytic sodium and chlorine precipitates. Formation of voids and their interactions with Na colloids and chlorine precipitates is often followed by a powerful chemical back-reaction between radiolytic sodium and chlorine, which results in a sudden fracture of the crystal and ultimately decomposition [9, 10]. To explain void formation in ionic crystals a new model of radiolysis has been proposed [11, 12], which includes the production of V_F centres (which are complex defects consisting of a cation vacancy with a self-trapped hole) at dislocations as a consequence of their reaction with excess H centres. Voids nucleate as a result of reactions between growing metallic colloids and halogen bubbles [11]. Subsequently, the voids continue to grow due to the formation of electro-neutral vacancy pairs, created during the reaction between F and V_F centres arriving at the void surface. V_F centre formation has no analogy in metals.

Another effect related to the chemical nature of point defects in NaCl is the formation of Na colloid nano-structures with one-dimensional (1D) magnetic behaviour [13–17]. Direct AFM measurements have revealed ring- and chain-like clusters (or agglomerates) of Na colloid particles which are situated very close to each other [18]. It appears that these structures are responsible for special magnetic properties of heavily irradiated samples. The only 1D structures in irradiated crystals which might provide nucleation sites for Na colloids are straight dislocations and dislocation loops. Therefore we propose that sodium colloids nucleate and grow along dislocations by a continued process of absorption of F centres, which are vacancy-type defects. In metals absorption of vacancies by a dislocation results only in dislocation climb. In the two component ionic crystal NaCl the excess flux of F centres to a dislocation results in agglomeration of F centres and the formation of Na colloids attached to this dislocation. This explanation is in contradiction with the existing models of radiolysis for NaCl, which are based on the postulate that the dislocation bias for H centres is larger than the mean bias of the system. In [18] the discrepancy is explained by the fact that the dislocation bias depends on dislocation arrangement, i.e. the real dislocation structure in heavily irradiated materials is generally very inhomogeneous and contains various dislocation patterns such as pile-ups, walls etc. Dislocation forests can also be decorated by colloids, resulting in the formation of irregular fractal-like structures of colloids, which have been observed experimentally by means of AFM.

The volume fraction of metallic Na produced inside the sample during irradiation can be determined by measurements of either the stored energy (SE) or the latent heat of melting (LHM) of the Na colloids by differential scanning calorimetry (DSC). The DSC scans of the irradiated samples exhibit several melting peaks located at temperatures higher than 80 °C, i.e. the first peak is located below the melting temperature of bulk sodium. The total LHM in these peaks is an accurate measure of the amount of damage in the crystal [19]. Peak temperatures and shapes provide detailed information about the properties of the colloids. A comprehensive analysis of the DSC scans for samples with different irradiation doses has been presented in [20, 21]. For samples irradiated at a fixed temperature the LHM increases with irradiation dose. Recently, we have observed an interesting effect—the decrease of LHM during low-temperature irradiation (18 °C) of samples,

which has been irradiated before at a high temperature (100 °C), while in contrast with this the stored energy increases slowly. According to DSC measurements the LHM decreases due to dissolution of large colloids, because intensities of melting peaks decrease after low temperature irradiation.

The objectives of this paper are (i) to describe the simultaneous nucleation and growth of chlorine precipitates and sodium colloids in NaCl under high dose irradiation and (ii) to consider a mechanism of dissolution of large Na colloids during low temperature irradiation. We assume that the different behaviour of the LHM after low temperature irradiation is associated with the differences in the aggregation states of the sodium colloids. It is known that the main driving force for the microstructural evolution under irradiation is the difference between the capture efficiencies of H or F centres by extended defects of different kinds and/or sizes (Na colloids, chlorine inclusions and dislocations) [4, 11, 12]. During irradiation at high temperature (100 °C) the large colloids are in the liquid state, but at room temperature these colloids are in the solid state. For this reason their capture efficiencies differ, which might lead to observed dissolution of large colloids. In the next section we present some experimental details. Subsequently, the model and simulation results are described.

2. Experimental details

Synthetic NaCl single crystals doped with 300 ppm KBF_4 have been used for experimental studies. The reason for the choice of synthetic NaCl samples is that the kinetics of radiation damage accumulation in this material is similar to that in natural rock-salt. At the same time the synthetic NaCl crystals are more suitable for laboratory irradiation to high doses, because of higher mechanical stability as compared to natural rock-salt samples. The irradiation has been carried out with 0.5 MeV electrons in a linear accelerator up to 320 Grad at 100 °C. After the initial high temperature irradiation the samples were irradiated in the second stage at 18 °C to a maximum additional dose of 550 Grad. For each set of samples irradiated to the same dose the SE and the LHM of radiolytic sodium and chlorine precipitates have been measured with a Perkin-Elmer DSC-7 system. Figure 1 shows the dose dependence of sodium LHM and SE during the two-stage irradiation experiment. The LHM of sodium increases during the initial high temperature irradiation, whereas during the second stage irradiation at 18 °C the decrease of the LHM of sodium can be seen very clearly (figure 1(a)).

In figure 1(b) the dose dependence of the SE is plotted. The SE released during DSC measurements due to the back-reaction between radiolytic products is proportional to the total number of neutral sodium atoms created by irradiation in NaCl crystal lattice. The LHM of sodium/chlorine is proportional to the amount of sodium/chlorine agglomerated in sufficiently large particles, which exhibit the above-described melting behaviour. The left part of figure 1(b) shows the increase of the SE during irradiation at 100 °C. The SE values after low temperature irradiation demonstrate significant sample to sample dispersion.

Nevertheless, a small increase of the SE with irradiation dose can be noticed (at least there is no consistent decrease of the SE, figure 1(b)); at the same time the LHM of sodium decreases appreciably. Obviously, the decrease of LHM is due to dissolution of large colloids. The slow growth of SE with low temperature dose can be explained by nucleation of small sized Na clusters (which do not contribute to the melting peaks observed in these experiments), which appear to replace the above mentioned large, shrinking colloids. This means that under low temperature irradiation the size distribution of the colloids changes appreciably. As for the LHM of chlorine, there is a large scatter of experimental data points; therefore we are not in a position to conclude that the LHM of chlorine decreases in the same proportion as the LHM of sodium (figure 2).

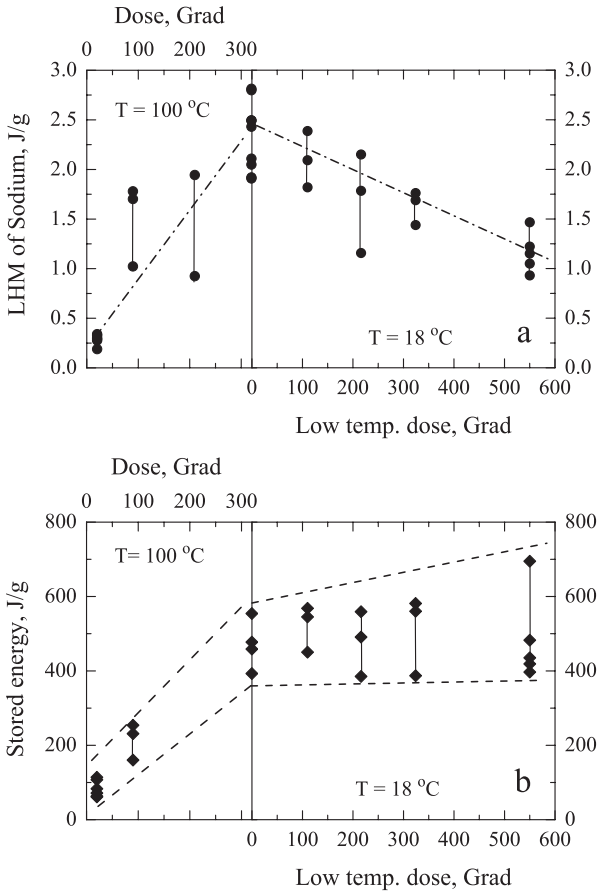

Figure 1. The LHM of sodium colloids (a) and the stored energy (b) versus dose in the two stage irradiation experiment. The dashed–dotted lines in (a) are plotted as a guide for the eyes. Data points connected by the solid lines correspond to sets of samples irradiated to the same high and low temperature doses. The dashed lines in (b) show the general trends for the minimum and maximum SE values.

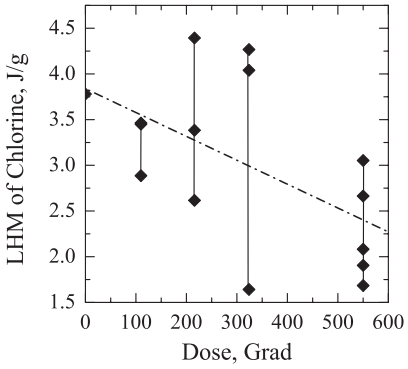

Figure 2. The LHM of chlorine precipitates versus the low temperature dose. The dashed–dotted line is a fit to the data. Data points connected by the solid lines correspond to sets of samples irradiated to the same high and low temperature doses.

3. The model

We will use a mean field approach to describe diffusion controlled clustering of radiation-induced F and H centres. In other words, we formulate a set of chemical rate equations for the average concentrations of mobile F and H centres and clusters of these defects. The traps for H centres are introduced in the model. Trapping of H centres by impurities is necessary to account for chlorine bubble nucleation, because the rate of homogeneous nucleation of chlorine bubbles is small due to the low concentration of highly mobile H centres [20, 22]. The nature of traps for H centres will not be specified. In principle, NaCl material can contain various types of traps with different binding energies with point defects. Crystal lattice defects, which may serve as traps for H and F centres, include impurity ions and complexes, dislocation jogs, grain boundaries etc. At present we have no detailed information on the nature of trapping centres in NaCl. Possibly a series of special low dose irradiation experiments involving samples with different concentrations of dopants could help to answer the question of the relation between defect traps and doping. However, this task is beyond the scope of the present paper. The aim of this paper is to find a physical mechanism of dissolution of large Na colloids during low temperature irradiation, using a minimum set of assumptions.

Since the concentration of radiation-induced F centres is relatively high, colloid nucleation is described by homogeneous coagulation of F centres to higher order clusters. The following reactions between traps, F centres, H centres and their clusters, F_n and H_n, are considered (note that some of the reactions are irreversible):

$$\begin{aligned}
&F_n + F \leftrightarrow F_{n+1}\\
&F_n + H \rightarrow F_{n-1}\\
&\mathrm{Trap} + H \leftrightarrow H^{\mathrm{T}}\\
&H^{\mathrm{T}} + H \rightarrow H_2^{\mathrm{T}}\\
&H_n^{\mathrm{T}} + H \rightarrow H_{n+1}^{\mathrm{T}}\\
&H_n^{\mathrm{T}} + F \rightarrow H_{n-1}^{\mathrm{T}}.
\end{aligned}$$

The concentrations of F and H centres change with time according to

$$\begin{aligned}
\frac{\mathrm{d}C_{\mathrm{F}}}{\mathrm{d}t} &= K - \beta D_{\mathrm{H}} C_{\mathrm{H}} C_{\mathrm{F}} - 4\beta D_{\mathrm{F}} C_{\mathrm{F}}^2 - \beta D_{\mathrm{F}} C_{\mathrm{F}} C_{\mathrm{HT}} + W_{\mathrm{C}}^{-}(2) C_2\\
&\quad - D_{\mathrm{F}} C_{\mathrm{F}} k_{\mathrm{F}}^2 + D_{\mathrm{F}} \frac{4\pi}{\omega} \sum_{n=2}^{\infty} r_n C_n Z_{\mathrm{CF}}(n) C_{\mathrm{F}}^{e}(n) \qquad (1)\\
\frac{\mathrm{d}C_{\mathrm{H}}}{\mathrm{d}t} &= K - \beta D_{\mathrm{H}} C_{\mathrm{H}} C_{\mathrm{F}} - \beta D_{\mathrm{H}} C_{\mathrm{H}} \left(C_{\mathrm{T}} - C_{\mathrm{HT}} - \sum_{n=2}^{\infty} B_n \right) - \beta D_{\mathrm{H}} C_{\mathrm{H}} C_{\mathrm{HT}}\\
&\quad - D_{\mathrm{H}} C_{\mathrm{H}} k_{\mathrm{H}}^2 + \nu_{\mathrm{HT}} C_{\mathrm{HT}} \qquad (2)
\end{aligned}$$

where K is the production rate of F and H centres measured in terms of displacements per atom per second (dpa s^{-1}), β is the recombination rate constant, D_{H} and D_{F} are the diffusion coefficients of H and F centres, respectively, C_{T} is the concentration of traps for H centres, C_{HT} is the concentration of trapped H centres, C_n is the concentration of F_n clusters, B_n is the concentration of H_n clusters, W_{C}^{-} is the shrinkage rate coefficient of colloids (see below), ω is the atomic volume of the host lattice, r_n is the radius of the cluster containing n point defects, ν_{HT} is the de-trapping rate of H centres

$$\nu_{\mathrm{HT}} = \beta D_{\mathrm{H}} \exp\left(-\frac{E_{\mathrm{HT}}}{k_{\mathrm{B}} T} \right) \qquad (3)$$

$C_{\mathrm{F}}^{e}(n)$ is the thermal concentration of F centres in equilibrium with colloids containing n sodium atoms

$$C_{\mathrm{F}}^{e}(n) = \exp\left(\frac{2\gamma\omega}{k_{\mathrm{B}}Tr_n} - \frac{E_{\mathrm{Ff}}}{k_{\mathrm{B}}T}\right) \tag{4}$$

where γ is the colloid–matrix interface energy and E_{Ff} is the formation energy of F centres.

The total sink strength for absorption of point defects k_i^2 is given by

$$k_i^2 = \frac{4\pi}{\omega}\sum_{n=2}^{\infty} r_n\left(C_n Z_{\mathrm{Ci}}(n) + B_n Z_{\mathrm{Bi}}(n)\right), \qquad i = \mathrm{F}, \mathrm{H} \tag{5}$$

where Z_{Ci} and Z_{Bi} are the point defect capture efficiencies of sodium clusters (colloids = C) and chlorine clusters (bubbles = B).

Nucleation of chlorine precipitates starts from trapping of mobile H centres; the concentration of H centres at the traps obey the equation

$$\frac{\mathrm{d}C_{\mathrm{HT}}}{\mathrm{d}t} = \beta D_{\mathrm{H}}C_{\mathrm{H}}\left(C_{\mathrm{T}} - C_{\mathrm{HT}} - \sum_{n=2}^{\infty} B_n\right) + W_{\mathrm{B}}^{-}(2)B_2 - \beta C_{\mathrm{HT}}\left(D_{\mathrm{H}}C_{\mathrm{H}} + D_{\mathrm{F}}C_{\mathrm{F}}\right) - \nu_{\mathrm{HT}}C_{\mathrm{HT}} \tag{6}$$

where W_{B}^{-} is the shrinkage rate coefficient of chlorine precipitates (see below).

Continued trapping of F and H centres by dimers, trimers and higher aggregates leads to formation of a distribution of different cluster sizes

$$\frac{\mathrm{d}C_2}{\mathrm{d}t} = 2\beta D_{\mathrm{F}}C_{\mathrm{F}}^2 - \left(W_{\mathrm{C}}^{-}(2) + W_{\mathrm{C}}^{+}(2)\right)C_2 + W_{\mathrm{C}}^{-}(3)C_3 \tag{7}$$

$$\frac{\mathrm{d}C_n}{\mathrm{d}t} = W_{\mathrm{C}}^{+}(n-1)C_{n-1} - \left(W_{\mathrm{C}}^{-}(n) + W_{\mathrm{C}}^{+}(n)\right)C_n + W_{\mathrm{C}}^{-}(n+1)C_{n+1} \tag{8}$$

$$\frac{\mathrm{d}B_2}{\mathrm{d}t} = \beta D_{\mathrm{H}}C_{\mathrm{H}}C_{\mathrm{HT}} - W_{\mathrm{B}}^{-}(2)B_2 - W_{\mathrm{B}}^{+}(2)B_2 + W_{\mathrm{B}}^{-}(3)B_3 \tag{9}$$

$$\frac{\mathrm{d}B_n}{\mathrm{d}t} = W_{\mathrm{B}}^{+}(n-1)B_{n-1} - W_{\mathrm{B}}^{-}(n)B_n - W_{\mathrm{B}}^{+}(n)B_n + W_{\mathrm{B}}^{-}(n+1)B_{n+1}. \tag{10}$$

Sodium and chlorine clusters nucleate and evolve due to absorption of H and F centres. We also take into account the thermal emission of F centres from sodium clusters. The corresponding growth and shrinkage rate coefficients are defined as follows

$$W_{\mathrm{C}}^{+}(n) = \frac{4\pi}{\omega}r_n D_{\mathrm{F}}Z_{\mathrm{CF}}(n)C_{\mathrm{F}} \tag{11}$$

$$W_{\mathrm{C}}^{-}(n) = \frac{4\pi}{\omega}r_n\left(D_{\mathrm{H}}Z_{\mathrm{CH}}(n)C_{\mathrm{H}} + D_{\mathrm{F}}Z_{\mathrm{CF}}(n)C_{\mathrm{F}}^{e}(n)\right) \tag{12}$$

$$W_{\mathrm{B}}^{+}(n) = \frac{4\pi}{\omega}r_n D_{\mathrm{H}}Z_{\mathrm{BH}}(n)C_{\mathrm{H}} \tag{13}$$

$$W_{\mathrm{B}}^{-}(n) = \frac{4\pi}{\omega}r_n D_{\mathrm{F}}Z_{\mathrm{BF}}(n)C_{\mathrm{F}}. \tag{14}$$

As distinct from other models [4, 12, 20, 22] the model presented in this paper does not contain dislocations explicitly. In the literature isolated dislocations in NaCl are assumed to be biased to absorption of H centres, and dislocations are considered to be necessary microstructural elements of the radiolysis process. However, below we will see that radiolysis is possible in a dislocation free material. The driving force is the asymmetry in absorption of H and F centres by clusters of different sizes and types. On the other hand, dislocations may provide nucleation sites both for bubbles and colloids [18].

It is known that other defects, such as V_F centres, voids and dislocation loops, can be formed in NaCl under irradiation. To keep the model simple we have not included these defects in the model. Several remarks should be made about these defects. As a result of absorption of excess H centres by dislocations V_F centres can be produced [11, 12]. The V_F centre can be considered as a bound vacancy pair (electro-neutral Schottky pair) occupied by a Cl atom. Absorption of V_F centres by growing bubbles reduces the stress associated with agglomeration of H centres (interstitial Cl atoms). A more efficient mechanism of stress relaxation is loop punching. In chemical reactions between growing colloids and halogen bubbles voids are formed, which grow by absorption of F and V_F centres [12]. However, according to our previous papers the sink strength of voids is smaller than the sink strengths of colloids and bubbles. This means that voids are secondary defects and do not influence essentially the evolution of colloids and chorine precipitates. It is known that growing colloids have a negative size misfit with the NaCl matrix [20]. The negative size misfit can be accommodated by absorption of dislocation loops that were punched from growing chlorine precipitates. Another mechanism of size misfit reduction at elevated temperatures is the formation of electro-neutral vacancy pairs (Schottky pairs) at the colloid–matrix interface, since, according to experimental data [24] and calculations [25], the energy of their formation is about 1.2–1.3 eV, which is not very high. At irradiation temperatures higher than the melting temperature of sodium, the size misfit can be decreased by formation of microvoids attached to the liquid colloid. Evaporation of bound Schottky pairs from these microvoids is enhanced due to the small size of the microvoids (Gibbs–Thomson effect).

The discussion presented above shows that interactions between point defects and radiolytic products are very complex. Therefore, to meet the objective of this paper we use a simplified model. Later, other defects and microstructural elements can be incorporated in the model.

The driving force of radiolysis is the difference of the fluxes of F and H centres to different sinks; i.e., on average, bubbles should be biased to absorption of H centres. The efficiency of a defect cluster to capture particular point defects depends on the interaction of these point defects with the cluster. The interaction results in a net drift of point defects to the cluster in addition to the diffusion flux. The flux of point defects to the defect cluster is given by

$$J_A = 4\pi R Z_{Ai} D_i C_i; \quad A = \text{Bubble, Colloid}; \quad i = \text{F, H}. \tag{15}$$

The calculation of capture efficiencies is a separate and complicated task. For metals this problem has received much attention in the past in connection with the problem of vacancy swelling of structural materials of nuclear reactors. Generally, the capture efficiency of the isolated spherical macrodefect of radius R is given by [11, 23]

$$Z_{Ai}(R) = 1 + \alpha_{Ai}^{(1)} \frac{a}{R} + \alpha_{Ai}^{(2)} \frac{\sigma_n}{\mu} + \alpha_{Ai}^{(3)} \left(\frac{\sigma_n}{\mu} \right)^2 \tag{16}$$

where a is the lattice constant, $\alpha_{Ai}^{(n)}$ are the dimensionless constants which depend on the material properties and temperature, σ_n is the normal stress at the cluster–matrix interface and μ is the shear modulus of the matrix. The origin of various terms in this formula is discussed in [11, 23]. In dense pile-ups or bunches of macrodefects the capture efficiencies also depend on the arrangement of microstructural defects, since the elastic field of clusters may overlap, i.e. a point defect may interact with several clusters simultaneously [26]. Rather than going into details of the capture efficiency calculations, in our simulations we will use model dependences of capture efficiencies on temperature and cluster size.

Schematically, the mechanism of colloid dissolution at low temperature can be described as follows. The number of F centres n in a large colloid changes with time

$$\frac{\mathrm{d}n}{\mathrm{d}t} \propto (\delta_{\mathrm{mean}} - \delta_{\mathrm{C}}(n))\, D_{\mathrm{F}} C_{\mathrm{F}} \tag{17}$$

where the bias of colloids for absorption of H centres $\delta_{\mathrm{C}}(n)$ is defined by

$$\delta_{\mathrm{C}}(n) = 1 - \frac{Z_{\mathrm{CF}}(n)}{Z_{\mathrm{CH}}(n)} \tag{18}$$

and the mean bias of the system δ_{mean} is determined by all macrodefects present in the system

$$\delta_{\mathrm{mean}} = 1 - \frac{k_{\mathrm{F}}^2}{k_{\mathrm{H}}^2}. \tag{19}$$

During irradiation at a high temperature the large colloids are in a liquid state (according to DSC the melting temperatures of colloids are distributed in the interval from 80 to 140 °C [20]). At high temperatures $\delta_{\mathrm{mean}} - \delta_{\mathrm{C}}(n) > 0$; i.e. $\mathrm{d}n/\mathrm{d}t > 0$. At low temperatures, because of solidification, the absolute value of the size misfit of these colloids increases. This means that at low temperatures the bias for absorption of H centres by large colloids may become larger than the mean bias of the system, i.e. large colloids should shrink: $\delta_{\mathrm{mean}} - \delta_{\mathrm{C}}(n) < 0$ and $\mathrm{d}n/\mathrm{d}t < 0$. The linear expansion of bulk sodium upon melting is about 0.9%. Assuming that the liquid colloid has no or very small size misfit, which does not contribute to the capture efficiencies ($\alpha_{\mathrm{Ai}}^{(2)}\sigma_n/\mu \ll 1$), and taking into account the linear thermal expansion of the NaCl matrix and the colloid, the size misfit, ε, of the solid colloid with the BCC lattice of bulk sodium is about -1%. This negative misfit results in tensile stresses inside the colloid and in a stronger interaction of H centres with the colloid as compared with F centres; i.e., at low temperatures large colloids are expected to absorb preferentially H centres. The term $\alpha_{\mathrm{Ai}}^{(2)}\sigma_n/\mu$ in the expression for the capture efficiency (16) is responsible for this effect. The normal stress at the cluster–matrix interface is given by

$$\sigma_n = \frac{12\mu K_{\mathrm{C}}}{4\mu + 3K_{\mathrm{C}}}\varepsilon, \qquad \sigma_n/\mu = -0.011, \tag{20}$$

where K_{C} is the colloid bulk modulus. In metals the value of the coefficient $\alpha_{\mathrm{Ai}}^{(2)}$ is usually between about 1 and 10 [23]. We assume that one is dealing with similar values in the case of NaCl. This means that the colloid bias might change considerably after cooling down the sample from 100 °C to room temperature. As for small colloids, it is likely that they do not exhibit melting, since the surrounding matrix forces the Na atoms to retain the FCC lattice of the Na sublattice [21], similar to small lithium precipitates in lithium fluoride [27]. Therefore we expect that the temperature dependence of their bias is weak.

4. Simulation results

To solve the kinetic equations (1), (2) and (6)–(10) we use the numerical method described in [28]. In order to reduce the number of equations we keep the original finite difference set of equations up to some reasonable number of atoms in the clusters; for larger sizes, the discrete equations (8), (10) are transformed to partial differential equations of the Fokker–Planck type for a continuous size variable, which allows coarse-graining of the numerical mesh. The combined set of equations—the discrete equations and the continuous Fokker–Planck equation—is solved numerically by the method of lines [29].

In simulations we used a standard set of material parameters [12, 20, 22] (table 1). We have found that the rate of colloid nucleation strongly depends on colloid–matrix interface energy. To overcome this difficulty we used the temperature dependent surface energy of colloids (table 1). This can be justified by the following known facts [30–32]: (i) with increasing temperature the

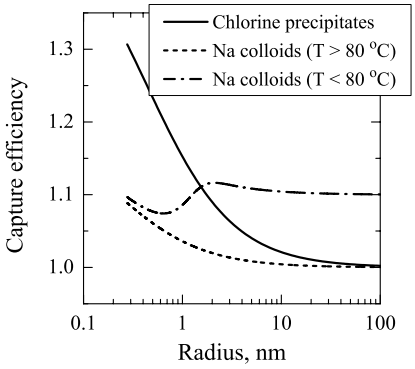

Figure 3. Capture efficiencies of H centres. It is assumed that small colloids (R<1 nm) are always solid and their capture efficiencies do not depend on the temperature.

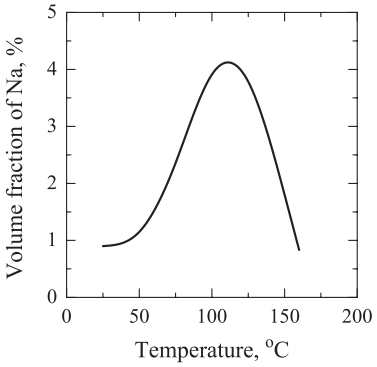

Figure 4. Simulated temperature dependence of volume fraction of radiolytic sodium after irradiation to 320 Grad.

Table 1. Material parameters used in calculations.

Parameter	Value
Absorbed energy required per primary F–H displacement (eV)	100
Dose rate, K, Mrad h^{-1} (dpa s^{-1})	480 (8×10^{-6})
Irradiation dose at 100 °C, Grad (dpa)	320 (19.4)
Irradiation dose at 20 °C, Grad (dpa)	550 (33.3)
Diffusion coefficient of H centres, D_H (m^2 s^{-1})	$10^{-6} \exp(-0.1\ eV/k_B T)$
Diffusion coefficient of F centres, D_F (m^2 s^{-1})	$10^{-6} \exp(-0.78\ eV/k_B T)$
Formation energy of F centres, E_{Ff} (eV)	1
Recombination rate constant, β (m^{-2})	3×10^{20}
Atomic volume of the host lattice, ω (m^{-3})	4.4×10^{-29}
Concentration of traps for H centres, C_T	10^{-5}
Binding energy of an H centre with the trap, E_{HT} (eV)	0.6
Colloid–matrix interface energy, $\gamma(T) = \gamma_0 + a(T - T_0)$ (mJ m^{-2})	430–0.4 (T − 373 K)
Colloid bulk modulus, K_C (GPa)	6.3
Shear modulus of NaCl, μ (GPa)	12.61

surface energy of solids decreases by about 0.5 mJ m^{-2} K^{-1} for many metals; and (ii) the surface energy of solids is higher than the surface energy of liquids.

For simplicity the capture efficiencies of F centres by bubbles and colloids are assumed to be equal to unity. The capture efficiencies of H centres by colloids and chlorine precipitates (figure 3) were adjusted to reproduce the experimental results of the second stage irradiation at low temperature. The input parameters were selected also to obtain the temperature dependence of Na volume fraction, which is typically observed experimentally (figure 4).

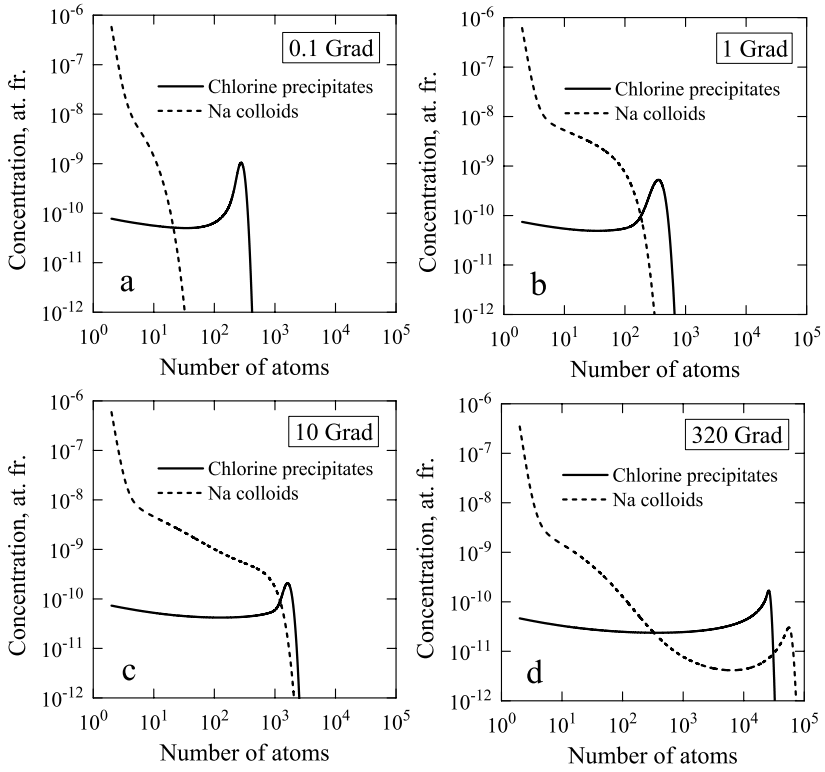

Figure 5. The development of the size distribution of the precipitates as a function of the irradiation dose. The concentrations of clusters C_n and B_n, denoted in the figure as Na colloids and chlorine precipitates, versus number of atoms n in clusters. The simulations correspond to irradiation at 100 °C up to 320 Grad (using the 'high temperature' capture efficiency for colloids, shown by a dashed line in figure 3).

Figure 5 shows the simulated formation of point defect clusters at 100 °C. Because of the high mobility of the H centres, chlorine clusters nucleate first. The leading edges of both distributions advance with time. We have checked that the contribution of homogeneous nucleation of chlorine clusters to the total volume fraction of radiolytic products is negligible. This explains the strong dependence of radiolysis on the amount and type of impurities, which is observed experimentally.

The dose dependences of the number densities and mean sizes of large clusters ($R >$ 0.5 nm) are plotted in figure 6. The concentration of small clusters ($R < 0.5$ nm) of Na is high, but their contribution to the volume fraction after irradiation at 100 °C is small. Figure 7 shows the dose dependence of the volume fraction.

The model sample, irradiated at 100 °C to a dose 320 Grad, was allowed to anneal for 1 week at 20 °C; no changes in volume fraction were observed, only the small-sized clusters ($n < 10$) annealed. Subsequently, the second stage irradiation at 18 °C to a maximum dose of 550 Grad was simulated using the 'low temperature' capture efficiency of the colloids (dash–dotted line in figure 3). The results are plotted in figure 8.

The size distribution functions $f_{B,C}(R, t)$ of the precipitates are defined in terms of their radii, which are related to concentrations of Na and chlorine clusters by

$$\int f_{\mathrm{B}}(R,t)\mathrm{d}R = \sum_n B_n, \qquad \int f_{\mathrm{C}}(R,t)\mathrm{d}R = \sum_n C_n, \qquad \frac{4\pi}{3}R^3 = n\Omega \tag{21}$$

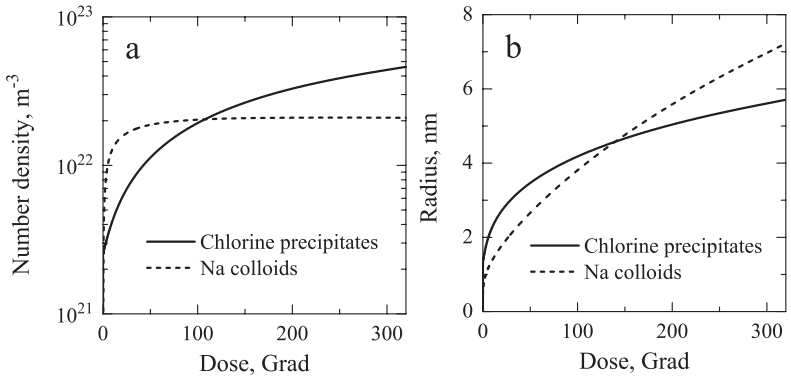

Figure 6. Simulated dose dependence of colloid and bubble parameters. The irradiation temperature is 100 °C.

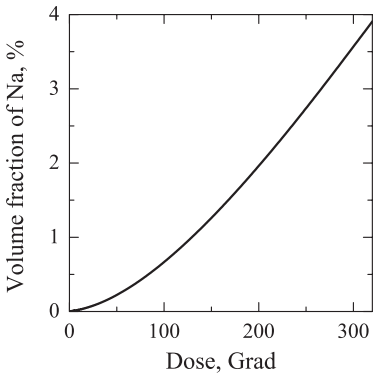

Figure 7. Simulated dose dependence of volume fraction of Na. The irradiation temperature is 100 °C.

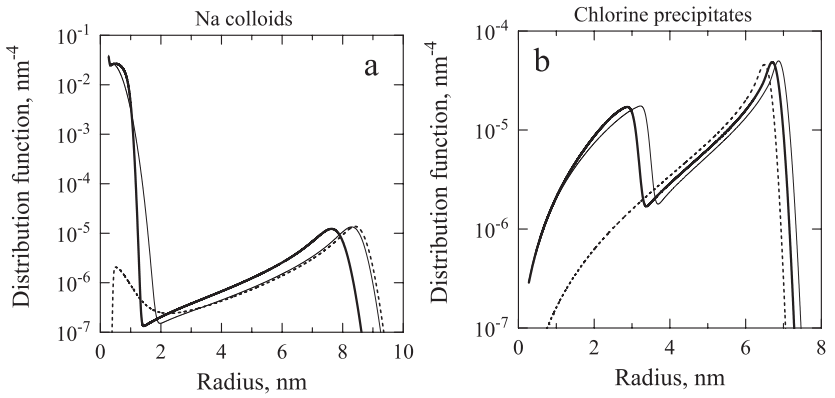

Figure 8. The simulated evolution of the distribution functions of Na colloids (a) and chlorine precipitates (b) after a second stage irradiation to 550 Grad at 18 °C. Initial distribution functions (dashed lines) were obtained by simulation of irradiation to 320 Grad at 100 °C. The thick solid lines correspond to calculations with the 'low temperature' capture efficiency of colloids (dash–dotted line in figure 3). Similar calculations with the 'high temperature' capture efficiency of colloids (dashed line in figure 3) are shown by the thin solid line.

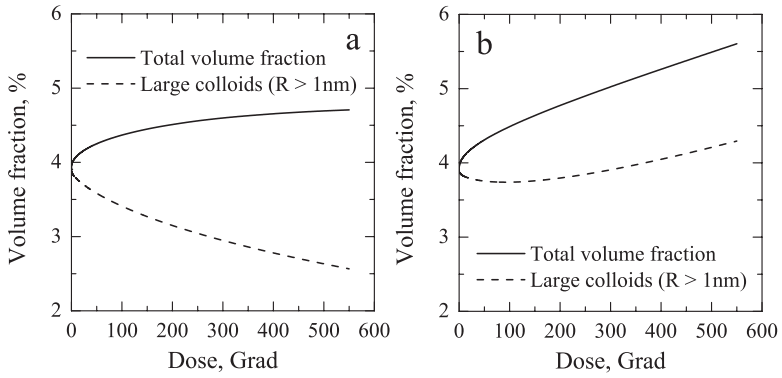

Figure 9. Total volume fraction of radiolytic Na (solid line) and the volume fraction of large colloids (dashed line) which exhibit melting behaviour. (a) Calculations with 'low temperature' capture efficiency of colloids (dash–dotted line in figure 3); (b) calculations with 'high temperature' capture efficiency of colloids (dashed line in figure 3).

where Ω is the mean atomic volume per atom in the clusters, which is about the same for sodium and chlorine clusters and close to the atomic volume of the host lattice $\Omega \approx \omega$.

Because of the high mobility of H centres, in the early stages of the low temperature irradiation a new population of chlorine clusters nucleates at available traps (which gives rise to the peak in figure 8(b) at about 3 nm), but as mentioned above its contribution to the total volume fraction is small. It can be seen that large colloids dissolve, while very large number densities of small colloids are predicted to nucleate.

Our explanation of the decrease of the LHM of sodium after low temperature irradiation is based on the different properties of solid and molten colloids. At low temperature (when the Na precipitates are in the solid state) we assume that the large colloids show an increased capture efficiency of H centres. To check this, similar calculations were performed for low temperature irradiation, while using the same H centre capture efficiencies as for molten colloids applied in the simulations of the high temperature irradiation experiments. The distribution functions for this case are shown by thin solid lines in figure 8. As expected, the changes of the size distribution of the large colloids are negligible. A very small shift of the distribution maximum to smaller sizes is due to the dissolution of colloids by highly mobile H centres at low doses (F centres are immobile at these doses).

The dose dependence of the volume fraction of the colloids is shown in figure 9. It is assumed that small colloids ($R < 1$ nm) do not contribute significantly to the LHM of Na. The fraction of large colloids distributed in the size interval 2 to 9 nm (figure 8) decreases in the calculations with the capture efficiency of the colloids, which is valid at 'low temperature' (figure 9(a)). For calculations with the 'high temperature' capture efficiency, the fraction of large colloids slightly decreases at low doses (<100 Grad) because of the dissolution of colloids by highly mobile H centres; however, at later stages both the total volume fraction and the fraction of Na in large colloids increase.

In figure 10 the results of the calculations are compared with experimental data. The model sample was 'irradiated' at 100 °C to a dose of 320 Grad. Then the second stage irradiation is given to the sample at 18 °C to a dose of 550 Grad in a simulation using the 'low temperature' capture efficiency of the colloids. According to figure 10, the agreement between the experimental results and the model predictions is satisfactory.

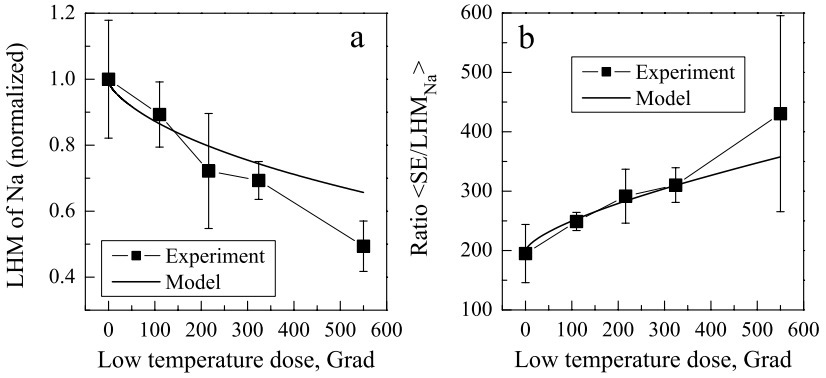

Figure 10. Comparison of simulation results with experimental data. The data points have been obtained by averaging the data depicted in figure 1(a) over a set of samples irradiated to the same high and low temperature doses. The error bars show the standard deviation $\sigma = \sqrt{\frac{1}{N}\sum_{i=1}^{N}(x_i - \bar{x})^2}$ for each set of experimental data. (a) The LHM (experiment) and the simulated volume fraction of large colloids ($R > 1$ nm). Both the experimental data and the data from simulations are normalized to the corresponding maximum values. (b) The ratio of SE to LHM of sodium (experiment) and the ratio of total amount of radiolytic Na to the amount of Na in large colloids ($R > 1$ nm). The latter is multiplied by the ratio SE/LHM = 195 measured in samples before low temperature irradiation.

5. Conclusions

- For the samples which had been irradiated in the first stage at a high temperature (100 °C) a decrease of the LHM has been revealed in the second stage irradiation at a low temperature (18 °C). In contrast with this, the stored energy (SE) increases slowly, indicating that the process of radiolysis continues.
- According to DSC measurements the defect structure reorganizes under low temperature irradiation: (i) the LHM decreases due to dissolution of large colloids under irradiation; (ii) at the same time the SE measurements show that a large volume fraction of small Na clusters is present.
- A model is formulated to describe the nucleation kinetics and the evolution of the size distribution of chlorine precipitates and sodium colloids in NaCl under high dose irradiation. It is proposed that the mechanism of dissolution of large Na colloids during low temperature irradiation can be related to the melting behaviour of sodium colloids.

Acknowledgment

The authors would like to thank NWO for their support by providing a visitor's grant to one of them (AAT).

References

[1] Chapman N A and McCombie C 2003 *Principles and Standards for the Disposal of Long-Lived Radioactive Wastes* (Amsterdam: Elsevier)

[2] EURADWASTE'04-Radioactive waste Management 2004 Community policy and research initiatives *Proc. 6th EC Conf. (Luxembourg, March–April 2004)* Publications Office of the European Communities, EUR 21027 EN

[3] Hobbs L W and Hughes A E 1975 Radiation damage in diatomic materials at high doses *Harwell Report AERE* R 8092

[4] Jain U and Lidiard A B 1977 The growth of colloid centers in irradiated alkali halides *Phil. Mag.* **35** 245–59

[5] Lidiard A B 1979 Energy stored in irradiated NaCl *Phil. Mag.* **39** 647–59

[6] den Hartog H W, Groote J C and Weerkamp J R W 1996 Stored energy in irradiated NaCl *Radiat. Eff. Defects Solids* **139** 1–19

[7] Vainshtein D I, Altena C and den Hartog H W 1997 Evidence of void lattice formation in heavily irradiated NaCl *Mater. Sci. Forum* **239–241** 607–10

[8] den Hartog H W and Vainshtein D I 1997 Explosive phenomena in heavily irradiated NaCl *Mater. Sci. Forum* **239–241** 611–4

[9] Vainshtein D I and den Hartog H W 2000 Explosive decomposition of heavily irradiated NaCl *Radiat. Eff. Defects Solids* **152** 23–37

[10] Turkin A A, Dubinko V I, Vainshtein D I and den Hartog H W 2002 A model for void-induced back reaction between radiolytic products in NaCl *Nucl. Instrum. Methods Phys. Res.* B **191** 83–8

[11] Dubinko V I, Turkin A A, Vainshtein D I and den Hartog H W 2000 Theory of the late stage of radiolysis of alkali halides *J. Nucl. Mater.* **277** 184–98

[12] Dubinko V I, Turkin A A, Vainshtein D I and den Hartog H W 2002 Kinetics of nucleation and coarsening of colloids and voids in crystals under irradiation *J. Nucl. Mater.* **304** 117–28

[13] Vainshtein D I and den Hartog H W 1996 ESR study of Na-colloids in heavily irradiated NaCl: size effects and inter-precipitate interactions *Appl. Radiat. Isot.* **47** 1503–7

[14] Cherkasov F G, Mustafin R G, L'vov S G, Khaibullin R I, den Hartog H W, Vainshtein D I and Vitol A Y 1998 Formation of the sodium 1D structures in doped NaCl by high energy electron irradiation *Vacuum* **51** 239–43

[15] Cherkasov F G, Mustafin R G, L'vov S G, Denisenko G A, den Hartog H W and Vainshtein D I 1998 Electron spin resonance and nuclear magnetic resonance of sodium macrostructures in strongly irradiated NaCl-K crystals: manifestation of quasi-one-dimensional behaviour of electrons *JETP Lett.* **67** 189–95

[16] Cherkasov F G, L'vov S G, Tikhonov D A, den Hartog H W and Vainshtein D I 2002 Metal-insulator and magnetic transitions in heavily irradiated NaCl-KBF_4 *J. Phys.: Condens. Matter* **14** 7311–9

[17] Cherkasov F G, L'vov S G, Tikhonov D A, den Hartog H W and Vainshtein D I 2002 The ground state of metallic nano-structures in heavily irradiated NaCl-KBF_4 *Radiat. Eff. Defects Solids* **157** 643–7

[18] Sugonyako A V, Turkin A A, Gaynutdinov R, Vainshtein D I, den Hartog H W and Bukharaev A A 2005 Systematic UHV-AFM experiments on Na nano-particles and nano-structures in NaCl *Phys. Status Solidi* c **2** 289–93

[19] Seinen J, Weerkamp J R W, Groote J C and den Hartog H W 1994 Radiation damage in NaCl. III. Melting phenomena of sodium colloids *Phys. Rev.* B **50** 9793–7

[20] Seinen J 1994 Radiation Damage in NaCl. The Process of Colloid Formation *PhD Thesis* Rijksuniversiteit Groningen

[21] Sugonyako A V, Vainshtein D I, Turkin A A, den Hartog H W and Bukharaev A A 2004 Melting of sodium clusters in electron irradiated NaCl *J. Phys.: Condens. Matter* **16** 785–98

[22] Groote J C and Weerkamp J R W 1990 Radiation damage in NaCl. Small particles *PhD Thesis* Rijksuniversiteit Groningen

[23] Borodin V A, Ryazanov A I and Abromeit C 1993 Void bias factors due to the anisotropy of the point defect diffusion *J. Nucl. Mater.* **207** 242–54

[24] Economou N A and Sastry P V 1964 High-temperature dielectric constant of NaCl and KBr *Phys. Status Solidi* **6** 135

[25] Tharmalingam K 1970 Calculation of energy of formation of vacancy pairs in alkali halides *J. Phys. C: Solid State Phys.* **3** 1856–60

[26] Turkin A A and Dubinko V I 1994 Formation of dislocation patterns under irradiation *Appl. Phys.* A **58** 35–9

[27] Lambert M, Mazieres Ch and Guinier A 1961 Precipitation de lithium dans les monocristaux de fluorure de lithium irradies aux neutrons thermiques *J. Phys. Chem. Solids* **18** 129–34

[28] Turkin A A and Bakai A S 2006 Formation of steady state size distribution of precipitates in alloys under cascade-producing irradiation *J. Nucl. Mater.* at press

[29] Schiesser W E 1991 *The Numerical Method of Lines: Integration of Partial Differential Equations* (New York: Academic)

[30] Adamson A W and Gast A P 1997 *Physical Chemistry of Surfaces* (New York: Wiley)

[31] Howe J M 1997 *Interfaces in Materials: Atomic Structure, Kinetics and Thermodynamics of Solid-Vapour, Solid-Liquid and Solid-Solid Interfaces* (New York: Wiley)

[32] Kumikov V K and Khokonov Kh B 1983 On the measurement of surface free energy and surface tension of solid metals *J. Appl. Phys.* **54** 1346–50